Available online at www.sciencedirect.com
SCIENCE DIRECT®
Marine Geology 198 (2003) 181–190
MARINE GEOLOGY
INTERNATIONAL JOURNAL OF MARINE GEOLOGY, GEOCHEMISTRY AND GEOPHYSICS
www.elsevier.com/locate/margeo

# Sediment surface effects on methane hydrate formation and dissociation

David Riestenberg [a], Olivia West [b,*], Sangyong Lee [b], Scott McCallum [b], Tommy J. Phelps [b]

[a] *Department of Geological Sciences, University of Tennessee, Knoxville, TN 37996-1410, USA*
[b] *Oak Ridge National Laboratory, Oak Ridge, TN 37831-6036, USA*

Accepted 13 February 2003

**Abstract**

The effects of sediment surfaces on methane hydrate formation and dissociation were investigated using colloidal suspensions and new experimental methods developed for a large volume (72 liters), temperature-controlled pressure vessel. Hydrates were formed by bubbling methane gas through test solutions at temperatures and pressures within the hydrate stability field. Hydrate formation was visually detected by the accumulation of hydrate-encrusted gas bubbles. To measure hydrate dissociation conditions, the pressure vessel was warmed while temperature was monitored within a zone of previously formed hydrate-encrusted gas bubbles. Hydrate dissociation was indicated by a distinct plateau in the hydrate zone temperature, while temperatures of the gas and liquid phases within the vessel continued to rise. The 'dissociation plateau' appears to be a phenomenon that is unique to the large volume of the pressure vessel used for the experiments. In experiments where hydrates were formed in pure water, temperature and corresponding pressure conditions measured during the temperature plateau matched model-predicted values for hydrate stability in water, thus confirming the validity of this new method for measuring hydrate dissociation conditions. Formation and dissociation conditions were measured for methane hydrates in colloidal suspensions containing bentonite. Hydrate formation experiments indicated that the presence of bentonite in water at 200 mg/l significantly decreased pressures required for hydrate formation relative to formation in pure water alone. On the other hand, hydrate dissociation conditions measured in bentonite and silica suspensions with solids concentrations of 34 g/l did not differ significantly from that of water. These results are relevant to the origin and stability of natural gas hydrate deposits known to exist in deep permafrost and marine sediments, where the effects of sediment surfaces are largely unknown.


*Keywords:* mineral surfaces; methane hydrates; gas hydrates; bentonite

## 1. Introduction

Gas hydrates are solid crystalline compounds that consist of low-molecular weight gases trapped in a framework of hydrogen-bonded

* Corresponding author. Tel.: +1-865-576-0505; Fax: +1-865-576-3989.
*E-mail address:* westor@ornl.gov (O. West).

0025-3227/03/$ – see front matter © 2003 Elsevier Science B.V. All rights reserved.
doi:10.1016/S0025-3227(03)00100-2

water molecules (Clarke et al., 1999). Because they are stable at low temperatures (< 10°C) and high pressures (> 3.5 MPa), methane hydrates naturally occur in the seafloor and permafrost sediment at thicknesses possibly exceeding 1 km (Milkov and Sassen, 2000). These deposits are considered a potential energy resource, containing 2–5 times the amount of methane in conventional gas sources (Kvenvolden, 1999). More recently, researchers have found evidence for rapid and massive hydrate dissociation in the geologic past that may be have been associated with global climate change (Hesselbo et al., 2000; Katz et al., 1999). Hydrate-bearing sediments may also be prone to slumping (Kvenvolden, 1999), therefore hydrates may represent a geotechnical hazard to offshore oil-rigs and platforms located in areas where sediment lies within the hydrate pressure–temperature (P–T) stability field.

Hydrate formation and equilibrium conditions in methane/water and methane/salt water systems are fairly well characterized (Sloan, 1998). However, there is a dearth of experimental data on hydrates formed in the presence of sediments where the pore structure and surface chemistry may influence equilibrium conditions (Clennell et al., 1999). A number of experiments on the influence of particle surface chemistry on hydrate formation have been reported in the literature. Blackwell (1998), for example, found that mineral surfaces that more closely mimic the crystal structure of water ice were effective hydrate nucleators, showing the greatest degree of kinetic promotion. Cha et al. (1988) and Ouar et al. (1992) observed a significant shift in the P–T stability curve of natural gas hydrate in bentonite (34 g/l) suspensions, suggesting the bentonite surfaces exhibited a thermodynamic effect. Englezos and Hall (1994) observed that $CO_2$ hydrate stability was unaffected by the presence of 5 g/l bentonite in water. Clearly, the effects of sediment surface chemistry are still largely unknown.

We addressed sediment surface effects by investigating methane hydrate formation and dissociation in suspensions of colloidal sediment minerals. These studies were conducted using new techniques in the Seafloor Process Simulator (SPS), a large volume high pressure vessel designed for gas hydrate research under natural ocean conditions (Phelps et al., 2001).

## 2. Materials and methods

The SPS is a large volume, temperature-controlled high pressure vessel capable of simulating deep seafloor pressures and temperatures where hydrates are stable (Fig. 1; Phelps et al., 2001). Details regarding the SPS (Fig. 1) can be found in Phelps et al. (2001). For the experiments reported here, the vessel pressure was measured using a series of piezoelectric transducers (Precise Sensors, model 9112) with a working range of 0–20 MPa (0–2900 psi). The vessel was cooled to experimental temperatures (2–7°C) in an explosion-proof cold room. Temperatures within the vessel were measured using Hastelloy-sheathed type K thermocouples (ARI Industries, Inc., Addison, IL) that were calibrated to an accuracy of ± 0.2°C. Thermocouples were placed in the gas phase, water phase, and at the gas–water interface where hydrates collected upon formation (Fig. 1B). Temperature and pressure data were collected in time sequence using a data acquisition system consisting of National Instruments Fieldpoint modules connected to a personal computer that logged data at 10–30-s time intervals using LabView v5.1.

Colloidal suspensions were prepared by premixing the colloids with a small amount of distilled water. These concentrated suspensions were then diluted to the experimental concentration using distilled water. The types of colloids used in the experiments included bentonite (Avocado, Ward Hill, MA, product No. 15795) and microcrystalline silica powder (Unimin, IMSIL microcrystalline silica A-8, Elco, IL), both with a median grain size of 3–5 μm.

Measurement of hydrate formation conditions was as follows. The vessel was filled with 55–57 l of water/colloid suspension leaving 15–20 l of gas headspace (Fig. 1B). In some experiments, polycarbonate spacer disks were attached to the vessel's top lid to lower the headspace volume to about 10 l. The vessel was then pressurized with 99.9% pure methane gas to about 3 MPa and

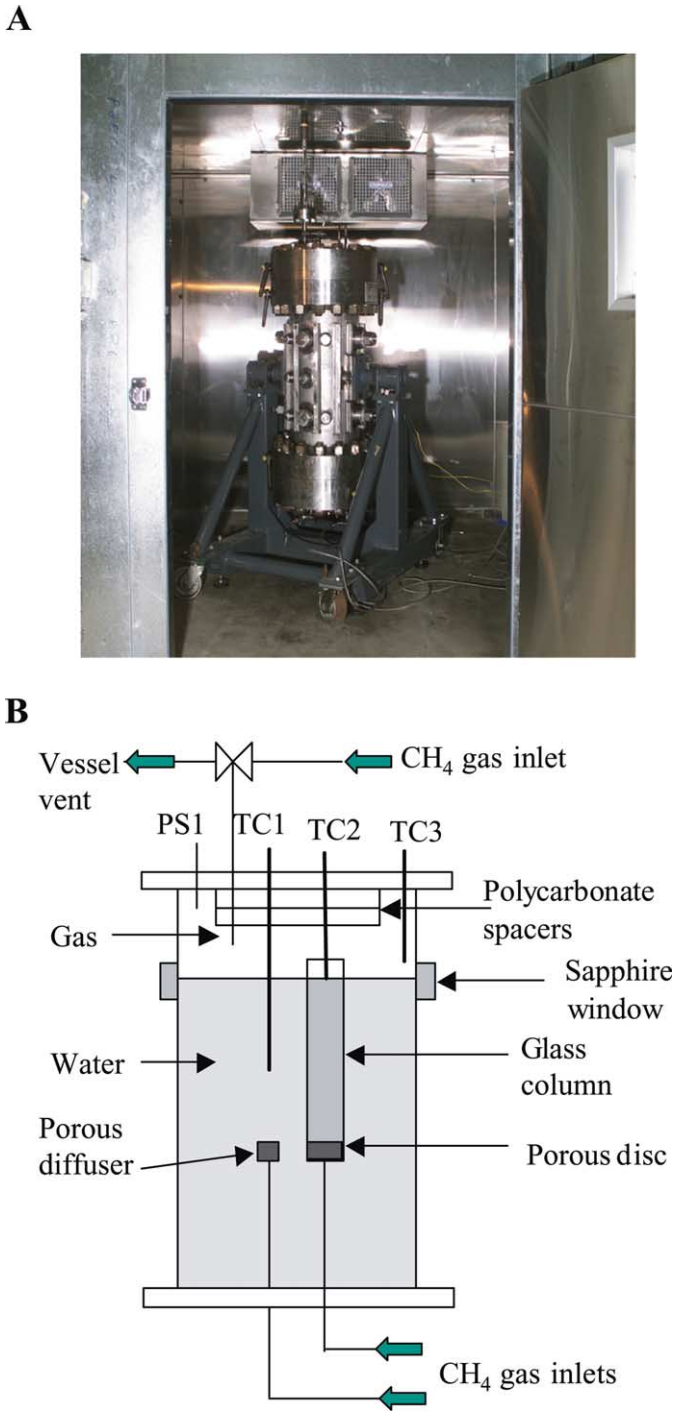


Fig. 1. (A) The SPS 70 at Oak Ridge National Laboratory. Photograph of the 41 port SPS and wheeled trunion mount within an explosion-proof temperature-controlled environmental chamber. (B) Schematic of the SPS indicating the location of sapphire windows, water phase, gas diffuser, experimental column, thermocouples (TC1–3), pressure transducer (PS1), and gas inlets and outlets.

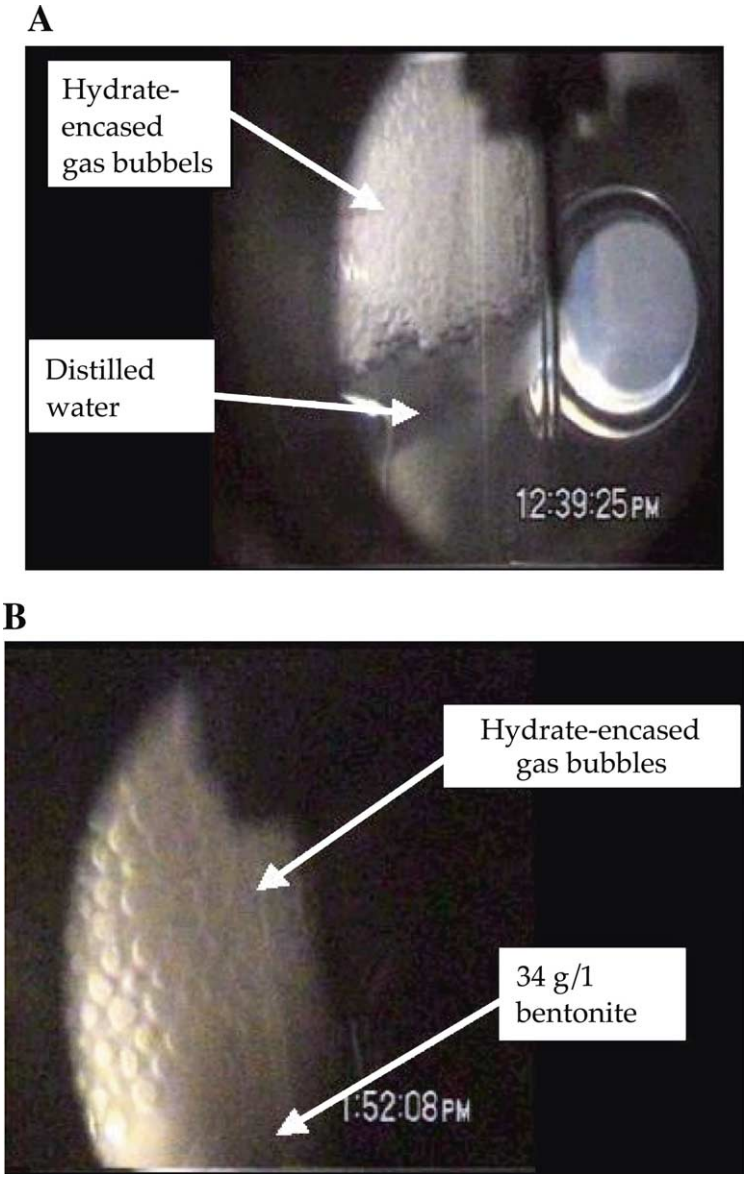


Fig. 2. Photograph hydrate-encased $CH_4$ collecting at the gas–water interface in a 4.8-cm-diameter column as seen through the sapphire windows of the SPS. (A) Hydrates formed at the gas–water interface in distilled water. (B) Hydrates formed in an aqueous suspension containing 34 g/l bentonite.

cooled to ~5°C for at least 12 h to allow the system to equilibrate outside of the bulk hydrate formation P–T conditions. After equilibration and with the vessel vent closed, methane gas was injected through a stainless steel porous diffuser at the bottom of the vessel. Alternatively, methane gas was injected through a 4.8-cm-diameter, 60-cm-long glass column containing the colloid/water suspension (Fig. 1). The glass column was used to ensure that the more concentrated colloidal suspensions were well homogenized during the gas injection. Gas was injected at a flow rate that

caused vessel pressure to increase at 0.041–0.048 MPa/min (6–7 psi/min). Prior to methane hydrate formation, gas bubbles would rise through the water and burst at the gas–water interface. Eventually, gas bubbles became encrusted with a methane hydrate film and began to accumulate at the gas–water interface (Fig. 2); the vessel pressure at this point was taken as the hydrate formation pressure. The vessel was depressurized to atmospheric conditions and flushed with nitrogen gas for a minimum of 2 h between each experiment to minimize memory effects (Sloan, 1998). No more than two experiments were performed without emptying the water from the vessel.

Hydrate dissociation equilibrium conditions were measured by warming the vessel after a mass of hydrates was produced following the procedure described above. After a mass of hydrate was formed, methane gas was either added or vented from the vessel headspace to achieve the target experimental pressure. The vessel vent was then closed and the vessel was warmed by turning the cold room refrigeration off, causing the gas and liquid in the vessel to warm at a rate less than 0.5°C/h. During this warming, the thermocouple in the hydrate zone at the gas–water interface would increase with time, but would eventually register a near constant value (a plateau) while the temperature of the vessel headspace continued to climb. The hydrate zone temperature plateau was considered an indication of hydrate dissociation; the temperature at the plateau and corresponding vessel pressure were taken as the hydrate stability P–T conditions.

## 3. Results and discussion

### 3.1. Formation

Hydrate formation during vessel pressurization was detected visually through the sapphire windows by the appearance of gas bubbles encrusted by a hydrate shell, which collected at the gas–water interface. Fig. 2 shows two views of hydrate formation in which semi-translucent bubbles can be seen collecting at the interface within the glass column. The bubble size for the water and colloid/water experiments ranged 3–5 mm in diameter, which was similar to the 2–6-mm bubble size created by Brewer et al. (1998) in their in situ ocean methane injection experiments. As the bulk volume of hydrate-encrusted gas bubbles increased, it would build downward into the water column and periodically the mass would migrate abruptly upward due to its buoyancy. Buoyancy differences between suspension and water-derived hydrates have not been quantified, although suspension-derived hydrates tended to exhibit less upward migration (data not shown).

Visual detection of hydrate formation was usually accompanied by a sharp increase in the interface temperature. This temperature jump was due to the exothermic nature of hydrate formation. The magnitude of the interface temperature increase ranged from 0.5°C for a small amount of hydrates up to 3°C if a massive amount was formed (data not shown).

It has been noted that in order to form hydrates, a system must be either overpressurized

Table 1
Observed hydrate formation pressures and estimated overpressurization and subcooling in water and bentonite (200 mg/l) suspensions

| Description of experiment | Experimental hydrate formation pressure (MPa) | Vessel temperature (°C; ±0.2°C) | Estimated hydrate formation overpressure (MPa) | Calculated hydrate formation subcooling (°C) |
|---|---|---|---|---|
| Water only | 8.96 | 4.0 | 5.37 | 8.4 |
| Water only | 8.61 | 6.0 | 4.13 | 6.2 |
| Bentonite 200 mg/l | 4.69 | 4.5 | 0.76 | 2.1 |
| Bentonite 200 mg/l | 4.53 | 4.6 | 0.69 | 1.7 |
| Bentonite 200 mg/l | 4.41 | 4.5 | 0.61 | 1.5 |
| Bentonite 200 mg/l | 4.38 | 4.5 | 0.58 | 1.5 |
| Bentonite averages ($n=4$) | 4.50 ± 0.14 | | 0.66 ± 0.08 | 1.7 ± 0.28 |

or subcooled to initiate hydrate formation (Englezos and Hall, 1994; Sloan, 1998; Morgan et al., 1999; Blackwell, 1998). In our experiments, the overpressurization necessary for hydrate formation dramatically decreased with the addition of colloids (Table 1). The estimated formation overpressurization is the difference between actual vessel pressure upon hydrate formation and the model-calculated (CSMHYD, Sloan, 1998) hydrate equilibrium pressure for pure water at the measured vessel temperature. The estimated formation subcooling is the difference between the actual vessel temperature and the model-calculated hydrate equilibrium temperature for pure water at the measured vessel pressure during hydrate formation. At 4–6°C, an overpressurization greater than 4 MPa was required to initiate hydrate nucleation in water (Table 1). The experiments with bentonite suspensions (200 mg/l) showed an average overpressurization of 0.66 MPa at temperatures similar to the water experiments. The small standard deviation between the repetition of these experiments (0.08 MPa) suggests that this phenomenon is highly reproducible.

Other researchers have noted a lowering of overpressurization or subcooling from bulk conditions of hydrate formation (Cha et al., 1988; Morgan et al., 1999; Blackwell, 1998). Our results suggest that even a relatively low (200 mg/l) concentration of suspended particulates has a significant effect on the kinetics of hydrate formation.

### 3.2. Dissociation

During the warming experiments, the temperature of the hydrates (at the interface) initially increased at the same rate as the water and headspace gas until it reached a point at which the gas–liquid interface temperature diverged from the gas temperature (Fig. 3; time ~10 h) and plateaued at a near constant value (Fig. 3; time ~12.5 h). The interface/hydrate zone temperature held steady over time as the temperature of the gas and liquid continued to rise. The near-constant temperature of the hydrate zone was interpreted as an indication of hydrate dissociation and absorption of the latent heat of hydrate formation. Over time, the interface temperature would again equilibrate and continue to rise with the gas phase temperature, presumably when hydrate dissociation was complete (Fig. 3; time ~20 h).

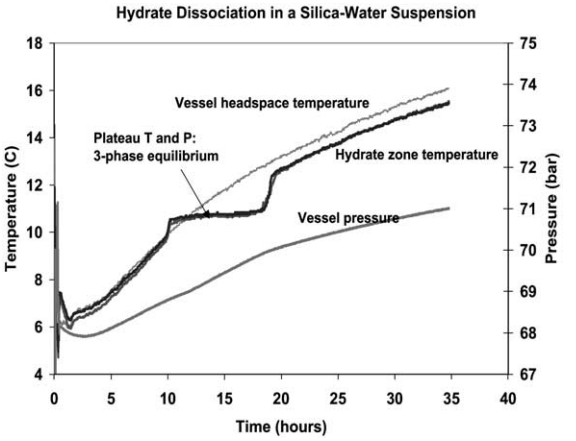


Fig. 3. Hydrate zone and gas phase temperatures and vessel pressure during vessel warming. Note that the interface/hydrate zone temperature plateaued for ~6 h while the gas phase temperature increased by 2°C during this same time period. The temperature plateau was attributed to the absorption of latent heat during hydrate dissociation.

Hydrate dissociation experiments were conducted in a closed vessel so, as expected, gas phase pressures measured in the vessel headspace initially increased with the gas phase temperature at a relatively constant rate (e.g. Fig. 3; time <10 h). Shortly after the hydrate zone temperature started to plateau, vessel pressure rose more rapidly with time, probably from gas released during hydrate dissociation (Fig. 3; time ~12.5 h). After the temperature plateau (Fig. 3; time ~20 h), the rate of increase of the vessel pressure markedly slowed, likely due to the end of hydrate dissociation such that subsequent pressure increase was from gas heating alone. The overall pressure change during a warming experiment was typically less than 1 MPa (10 bar), with the pressure change during the temperature plateau on the order of 0.1 MPa (1 bar). Thus, pressure was nearly constant during hydrate dissociation.

In all dissociation experiments a distinct plateau of the gas–water interface or hydrate temperature was evident, with the plateau duration rang-

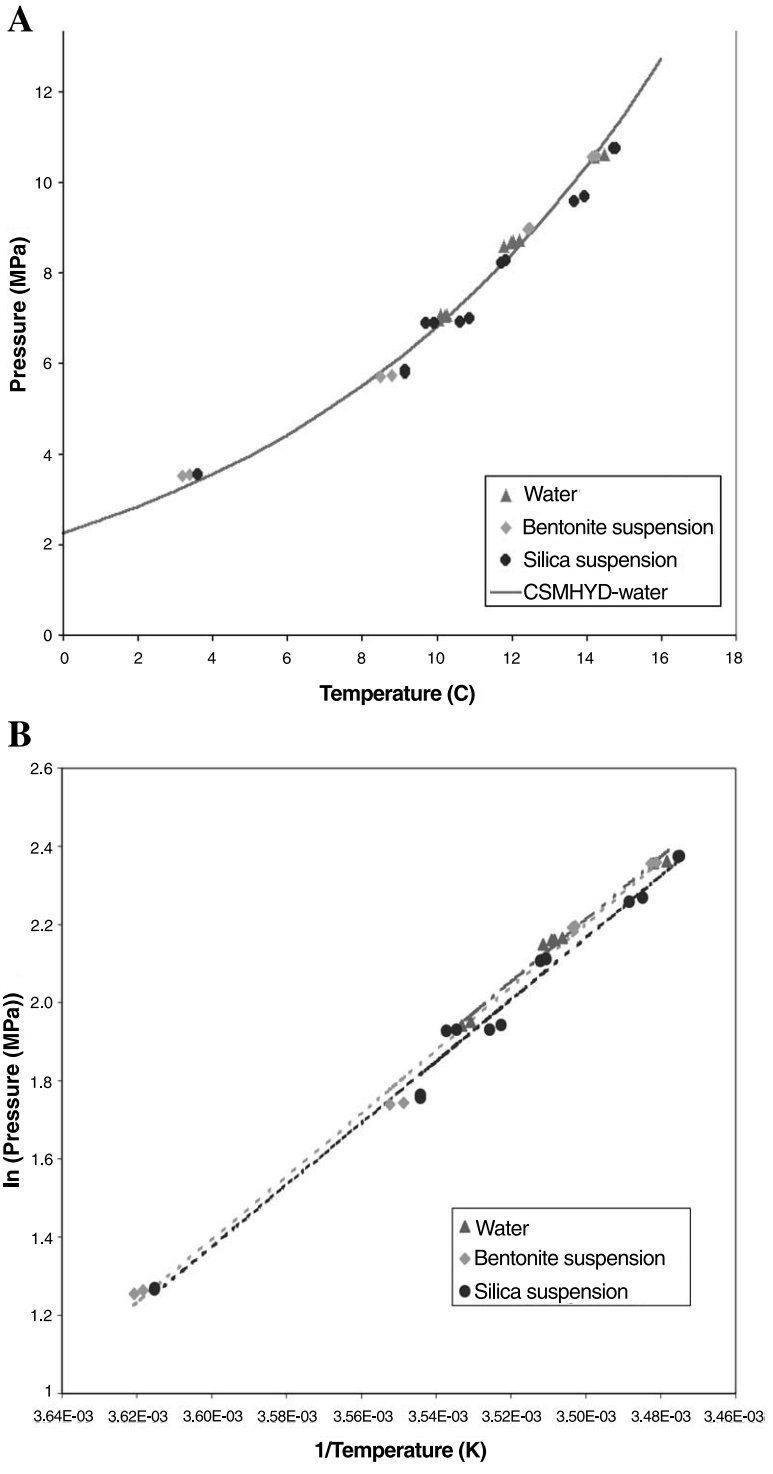


Fig. 4. (A) Comparison of CSMHYD model (Sloan, 1998) predictions with SPS hydrate equilibrium measurements. (B) Semi-logarithmic plot of P vs. 1/T (K) using same data as in (A).

ing from 0.7 h to as long as 9.5 h (Table 2). There were no distinct trends in the duration of the plateau with any of the experimental parameters. The plateau duration was likely affected by hydrate dissociation kinetics, the mass of hydrates produced, and the heating rate of the vessel. Because there was a limited degree of control in the amount of hydrates formed in our experiments, it is difficult to interpret the duration of the temperature plateaus listed in Table 2, although there appears to be a general trend of shorter plateau intervals at higher dissociation temperatures.

The long duration of the temperature plateaus seen in our experiments was probably a consequence of the large thermal mass of the vessel and its contents which allowed for gradual temperature increases and slow heat transfer as the vessel and its contents warmed. Furthermore, the relatively high volume of gas headspace in the vessel ($>10$ l) allowed for near-constant pressure conditions (change of $<0.1$ MPa) even while gas was released as hydrates dissociated. Thus, it was possible to achieve quasi-equilibrium between the hydrate, gas and liquid phases in the SPS during vessel warming. The endpoints of the temperature plateau and corresponding pressures were taken as hydrate–liquid–gas equilibrium conditions. We considered a plateau as occurring when the

Table 2
Characteristics of hydrate dissociation experiments and measured hydrate equilibrium pressures and temperatures

| Experiment/test solution | Dissociation temperature (C) | Dissociation pressure (MPa) | Duration of hydrate zone temperature plateau/hydrate dissociation (h) | Rate of temperature increase in hydrate zone during dissociation (C/h) | Rate of temperature increase in gas phase during hydrate dissociation (C/h) |
|---|---|---|---|---|---|
| Water | 10.0 | 6.97 | 5.8 | 0.03 | 0.24 |
| | 10.2 | 7.04 | | | |
| Water | 10.1 | 7.06 | 2.55 | 0.06 | 0.23 |
| | 10.3 | 7.08 | | | |
| Water | 11.8 | 8.58 | 9.5 | 0.03 | 0.18 |
| | 12.0 | 8.68 | | | |
| Water | 12.0 | 8.68 | 5.7 | 0.04 | 0.23 |
| | 12.2 | 8.73 | | | |
| Water | 14.2 | 10.56 | 1.4 | 0.21 | 0.44 |
| | 14.5 | 10.61 | | | |
| Water+34 g/l bentonite | 8.5 | 5.7 | 1.7 | 0.17 | 0.42 |
| | 8.8 | 5.72 | | | |
| Water+34 g/l bentonite | 12.4 | 8.96 | 2.0 | 0.03 | 0.35 |
| | 12.5 | 8.99 | | | |
| Water+34 g/l bentonite | 14.1 | 10.55 | 1.8 | 0.07 | 0.29 |
| | 14.3 | 10.58 | | | |
| Water+34 g/l silica | 3.6 | 3.55 | 1.76 | 0.01 | 0.61 |
| | 3.6 | 3.56 | | | |
| Water+34 g/l silica | 9.2 | 5.79 | 3.3 | 0.00 | 0.33 |
| | 9.2 | 5.83 | | | |
| Water+34 g/l silica | 9.6 | 6.87 | 1.49 | 0.15 | 0.25 |
| | 9.9 | 6.89 | | | |
| Water+34 g/l silica | 10.6 | 6.9 | 6.0 | 0.04 | 0.34 |
| | 10.9 | 7 | | | |
| Water+34 g/l silica | 11.73 | 8.23 | 2.38 | 0.05 | 0.21 |
| | 11.85 | 8.26 | | | |
| Water+34 g/l silica | 13.7 | 9.56 | 5.0 | 0.06 | 0.30 |
| | 14.0 | 9.67 | | | |
| Water+34 g/l silica | 14.7 | 10.74 | 0.74 | 0.04 | 0.20 |
| | 14.8 | 10.75 | | | |

temperature of the hydrates increased at a rate of $\leq 0.2$°C/h and when the rate of temperature increase of the hydrates differed visibly from that of the headspace gas. Measuring hydrate P–T equilibrium conditions during hydrate dissociation is an accepted technique used by several researchers, including Cha et al. (1988) and Maekawa et al. (1995). Wright et al. (1999), conducting warming experiments in a pressure vessel containing 100–140 $cm^3$ hydrate-bearing soil samples also found that the hydrate temperatures deviated from the vessel temperature for a period of 5–6 h, but the deviation did not approach a plateau.

Fig. 4A and Table 2 show P–T equilibrium measurements in distilled water, bentonite, and silica suspensions. Experiments with pure water gave equilibrium values consistent with model predictions for bulk water conditions (CSMHYD; Sloan, 1998). The bentonite and silica data as plotted in Fig. 4A did not show a significant effect on hydrate stability when compared to the experimental and CSMHYD-calculated equilibrium conditions for water. The shift in equilibrium for a 34 g/l bentonite suspension reported by Cha et al. (1988) and Ouar et al. (1992) was over 2°C vs. experiments conducted in pure water. They were using a natural gas mixture which contained $>10\%$ higher molecular weight hydrocarbons. Englezos and Hall (1994) reported that a 5 g/l bentonite suspension had little or no significant effect on $CO_2$ hydrate stability. P–T equilibrium conditions for the three test fluids are plotted in Fig. 4B on a semi-logarithmic graph with ln(P) and 1/T(K) on the $y$ and $x$-axis, respectively. The slopes of the fitted lines in Fig. 4B correspond to the heats of hydrate formation ($\Delta H_f$) for each of the test fluids through the Clausius–Clapeyron equation (Cha et al., 1988). The slopes of the fitted lines (with 95% confidence intervals) in Fig. 4B are $-7985 \pm 582$, $-9049 \pm 698$, and $-7910 \pm 474$ $K^{-1}$ for water, bentonite, and silica suspensions, respectively. The 95% confidence intervals were estimated as twice the standard error of the regressed slope. Using $d(\ln(P))/d(1/T) = -\Delta H_f/R$ where R is the gas constant, measured $\Delta H_f$ values are $66.4 \pm 4.8$, $75.2 \pm 5.8$, and $65.8 \pm 4.0$ kJ/mol for water, bentonite, and silica suspensions, respectively. $\Delta H_f$ values in the bentonite and silica suspensions are comparable to that of water alone. Differences between the water, bentonite and silica $\Delta H_f$ estimates is not statistically significant as their respective 95% confidence intervals overlap.

The fitted line through the silica data in Fig. 4B is shifted slightly relative to both the bentonite and water data. The relative shift between the bentonite and silica P–T curves may be interpreted as an increased ordering effect in the silica suspensions when compared to the bentonite suspensions. The silica powder consists of 98.5% quartz (analysis provided by supplier) while X-ray diffraction analysis of the bentonite showed a mixed mineral composition including smectite, illite, opal, quartz and plagioclase. Because water interacts differently with different mineral surfaces, our results suggest that there may be interactions between water molecules and the near-pure crystalline silica particles and the heterogeneous bentonite, and that the ordering on surfaces may favor hydrate formation at higher temperatures or lower pressures. With respect to dissociation, the effect of sediment surface chemistry appears to be statistically insignificant. Additional research is being conducted using purified water and a simulated natural gas for hydrate formation and stability studies.

## 4. Conclusion

We have developed a technique to examine the effects of particle concentration, type, and surface chemistry on hydrate formation and equilibrium conditions. Hydrate formation in water and colloidal suspensions were induced by bubbling methane gas through test solutions, and visually detected by the accumulation of hydrate-encased gas bubbles and the gas–water interface. The collected hydrate formation data show a dramatic impact of suspended particles, lowering the overpressure necessary for the onset of hydrate formation even at a relatively low solid concentration. Decreasing the required overpressurization could aid attempts to produce anthropogenic gas hydrates such as in ocean $CO_2$ sequestration or desalinization applications. To measure hydrate dis-

sociation conditions, the pressure vessel containing previously formed hydrates was warmed while temperature was monitored within the zone of hydrate-encrusted gas bubbles. Hydrate dissociation was then indicated by a distinct plateau in temperature within the hydrate zone, while temperatures of the gas and liquid phases within the vessel continued to rise. The latter appears to be a phenomenon that is unique to the large volume of the pressure vessel used for the experiments. The data collected suggest that some particle surfaces even at high concentrations have statistically insignificant impacts on methane hydrate stability. These results are in contrast to previously reported studies where bentonite was shown to significantly lower equilibrium pressure for a simulated natural gas which contained $>10\%$ higher molecular weight hydrocarbons (Cha et al., 1988; Ouar et al., 1992). Thus, for natural gas hydrate deposits that consist of nearly pure methane, stability may be little affected by sediment surface chemistries, whereas they may significantly decrease the overpressure required for hydrate formation.

## Acknowledgements

This research was supported by a grant from the Laboratory Director's Research and Development Fund of Oak Ridge National Laboratory and by the Gas Hydrates Program through the Office of Fossil Energy, U.S. Department of Energy. Oak Ridge National Laboratory is managed by UT-Battelle, LLC, for the U.S. Department of Energy under Contract No. DE-AC05-00-OR22725. We would also like to acknowledge the efforts of David Peters and Jim Blencoe in ORNL SPS operations. We also thank Yul Roh for performing the X-ray diffraction analysis.

## References

Brewer, P.G., Orr, F.M., Jr., Friedrich, G., Kvenvolden, K.A., Orange, D.L., 1998. Gas hydrate formation in the deep sea: In situ experiments with controlled release of methane, natural gas, and carbon dioxide. Energy Fuels 12, 183–188.

Blackwell, V.R., 1998. Formation Processes of Clathrate Hydrates of Carbon Dioxide and Methane. Ph.D. Thesis, California Institute of Technology, CA.

Cha, S.B., Ouar, H., Wildeman, T.R., Sloan, E.D., 1988. A third surface effect on hydrate formation. J. Phys. Chem. 92, 6492–6494.

Clennell, M.B., Hovland, M., Booth, J.S., Henry, P., Winter, W.J., 1999. Formation of natural gas hydrates in marine sediments, 1. Conceptual model of gas hydrate growth conditioned by host sediment properties. J. Geophys. Res. 104, 22985–23303.

Clarke, M.A., Pooladi-Darvish, M., Bishnoi, P.R., 1999. A method to predict equilibrium conditions of gas hydrate formation in porous media. Ind. Eng. Chem. Res. 38, 2458–2490.

Englezos, P., Hall, S., 1994. Phase equilibrium data on carbon dioxide hydrate in the presence of electrolytes, water soluble polymers and montmorillonite. Can. J. Chem. Eng. 72, 887–893.

Hesselbo, S.P., Grocke, D.R., Jenkyns, H.P., Bjerrum, C.J., Farrimond, P., Morgans-Bell, H.S., Green, O.R., 2000. Massive dissociation of gas hydrate during a Jurassic oceanic anoxic event. Nature 406, 392–395.

Katz, M.E., Pak, D.K., Dickens, G.R., Miller, K.G., 1999. The source and fate of massive carbon input during the latest Paleocene thermal maximum. Science 286, 1531–1533.

Kvenvolden, K.A., 1999. Potential effects of gas hydrate on human welfare. Proc. Natl. Acad. Sci. 96, 3420–3426.

Maekawa, T., Itoh, S., Sakata, S., Igari, S.-I., Imai, N., 1995. Pressure and temperature conditions for methane hydrate dissociation in sodium chloride solutions. Geochem. J. 29, 325–329.

Milkov, A.V., Sassen, R., 2000. Thickness of the gas hydrate stability zone, Gulf of Mexico Continental Slope. Mar. Pet. Geol. 17, 981–991.

Morgan, J.J., Blackwell, V.R., Johnson, D.E., Spencer, D.F., North, W.J., 1999. Hydrate formation from gasseous $CO_2$ and water. Env. Sci. Tech. 33, 1448–1452.

Ouar, H., Cha, S.B., Wildeman, T.R., Sloan, E.D., 1992. The formation of natural gas hydrates in water-based drilling fluids. Trans. IchemE. A 70, 48–54.

Phelps, T.J., Peters, D.J., Marshall, S.L., West, O.L., Liang, L., Blencoe, J.G., Alexiades, V., Jacobs, G.K., Naney, M.T., Heck, J.L., Jr., 2001. A new experimental facility for investigating the formation and properties of gas hydrates under simulated seafloor conditions. Rev. Sci. Instrum. 72, 1514–1521.

Sloan, E.D., 1998. Clathrate Hydrates of Natural Gases, 2nd. ed. Marcel Dekker, New York.

Wright, J.F., Dallimore, S.R., Nixon, F.M., 1999. Influences of grain size and salinity on pressure–temperature thresholds for methane hydrate stability in JAPEX/JNOC/GSC Mallik 2L-38 Gas Hydrate Research-Well sediments. In: Dallimore, S.R., Uchida, T., Collett, T.S. (Eds.), Results from JAPEX/JNOC/GSC Mallik 2L-38 Gas Hydrate Research-Well, Mackenzie Delta, Northwest Territories, Canada. GSC Bulletin 544, pp. 229–240.